



Wake redirection at higher axial induction

Carlo Cossu

Laboratoire d'Hydrodynamique Énergetique et Environnement Atmosphérique (LHEEA)
CNRS - Centrale Nantes, 1 rue de la Noë 44300 Nantes, France

Correspondence: Carlo Cossu (carlo.cossu@ec-nantes.fr)

Abstract. The energy produced by wind plants can be increased by mitigating the negative effects of turbine-wakes interactions. In this context, axial induction control and wake redirection, obtained by intentionally yawing or tilting the rotor axis away from the mean wind direction, have been the subject of extensive investigations. We have recently shown that the combination of static tilt control with static axial over-induction results in significant power gains. However, these early results were based on idealized turbine models where wake-rotation effects, radial force distributions and realistic turbine controller effects were neglected. In this study we therefore compute power gains that can be obtained by operating tilted rotors at higher axial induction for the more realistic native NREL 5-MW turbine model implemented in SOWFA. We then extend this approach to the case of yaw control. We show that power gains obtained by standard wake redirection based on yaw or tilt control are highly enhanced when the yawed or tilted turbines are operated at higher axial induction. These results confirm our early findings for the case of tilt control and extend them to the case of yaw control suggesting an high potential for the practical application of overinductive wake redirection.

1 Introduction

In wind farms, wind turbines shadowed by the wakes of other upwind turbines experience a decrease of the mean available wind speed and an increase of turbulent fluctuations resulting in decreased extracted wind power and increased fatigue loads (see Stevens and Meneveau, 2017; Porté-Agel et al., 2019, for a review). In currently installed wind farms, however, each turbine is typically operated in “greedy” mode maximizing its own individual power production. As the greedy operation mode does not generally lead to the global optimal, where the energy production of the whole wind farm is maximized (see e.g. Steinbuch et al., 1988), a number of different approaches have been proposed where the collective control of all turbines is used to increase the power production of the whole wind farm by mitigating the negative effects of turbine-wake interactions (see Knudsen et al., 2015; Boersma et al., 2017, for a review). Among the many proposed approaches, two have received particular attention: axial induction control and wake redirection control which can be static (the control is steady if the incoming wind conditions are) or dynamic (the control can be unsteady even for steady incoming wind conditions).



In axial induction control the induction factors of selected (usually upwind) turbines are steered away from the greedy operation mode in order to increase the power production of other (usually downwind) turbines. While static axial induction control has not demonstrated significant power gains in realistic settings (Knudsen et al., 2015; Annoni et al., 2016), dynamic axial induction control has shown promise for significant power gains (Goit and Meyers, 2015; Munters and Meyers, 2017). In wake redirection control the intentional misalignment of rotor axes from the wind direction is used to deflect turbine wakes in the horizontal or in the vertical direction by acting on yaw or tilt angles respectively with a documented increase of the global power produced by the wind farm (Dahlberg and Medici, 2003; Medici and Alfredsson, 2006; Jiménez et al., 2010; Fleming et al., 2014, 2015; Campagnolo et al., 2016; Howland et al., 2016; Bastankhah and Porté-Agel, 2016).

In two recent studies (Cossu, 2020a, b) we have shown that an appropriate combination of (static) tilt and (static) axial induction control results in a significant enhancement of the global power gains obtained in spanwise-periodic wind-turbine arrays. In particular, power gains were observed to be highly enhanced (up to a factor of 2 or 3) when the turbines with rotor tilted by the optimal angle ($\varphi \approx 30^\circ$) were operated at disk-based thrust coefficient $C'_T = 3$ higher than in the baseline case ($C'_T = 1.5$).

These early results (Cossu, 2020a, b) were obtained with an actuator-disk model where wake-rotation and the radial distribution of actuator-disk forces were neglected and the turbines were assumed to operate at constant given C'_T . This highly idealized setting, used in many previous investigations (e.g. Calaf et al., 2010; Goit and Meyers, 2015; Munters and Meyers, 2017), has been instrumental in obtaining general results not depending on the specific turbine control law and blade design but calls for confirmation on more realistic turbine models. Hence, a first goal of this study is to determine the power gains that can be obtained with high-induction (overinductive) tilt control when realistic turbine models are used that take into due account blade-design, wake-rotation and controller specificities. This goal is addressed in the first part of this study, by making use of SOWFA's (Churchfield et al., 2012) native actuator disk model for the NREL 5-MW turbine. In this implementation of the turbine model the radial dependence of the actuator disk force as well as wake rotation and C'_T are computed from turbine blades properties and NREL 5-MW's five-region realistic controller (Jonkman et al., 2009) is used.

In the second part of the study we address the case of yaw control. Indeed, the increased power gains obtained by operating tilted turbines at higher thrust coefficients mostly result from the increase of wake deviations obtained without a penalization of the power production of the tilted turbine. Overinductive wake deflection could therefore be beneficial also in the case of yaw-control where it is known that higher thrust coefficients also result in larger wake deviations (Jiménez et al., 2010; Howland et al., 2016; Shapiro et al., 2018). Surprisingly, however, only a few studies have investigated the potential benefits of combining axial induction control and yaw control: Park and Law (2015) show that significant power gains can be obtained in this way, based on simplified wake models and advanced optimization techniques, but they do not analyze the respective effects of yaw and induction while Munters and Meyers (2018) find that high power gains result from the combination of *dynamic* yaw and axial induction control and highlight the potential of quasi-static yaw control in the overinductive regime.

The second, probably most important, objective of the present study is therefore to ascertain if significant power gains can be obtained, with a combination of static yaw control and static axial induction control, by operating yawed turbines at higher axial induction.



The potential of overinductive wake redirection will be investigated by computing power gains that can be obtained in a
60 wind-turbine array composed of two spanwise-periodic rows of wind-aligned turbines where the same control is applied to all
upwind-row turbines while downwind-row turbines are left in default operation mode. This idealized configuration, which is an
extension to the spanwise-periodic case of the two-turbine configuration considered by Fleming et al. (2015), is chosen in order
to keep simple the physical interpretation of the results by isolating the effects of tilt or yaw angle and axial induction of the
upwind turbines without entering the problem of the optimization of these parameters in multi-row configurations. Importantly,
65 the relevance of these power gains will be tested without excessive assumptions by means of large-eddy simulations in the
atmospheric boundary layer using a turbine model which includes the effects of wake-rotation, radial force distribution and a
realistic turbine controller.

We anticipate that substantial enhancements (up to a factor of 3) of the power gains induced by wake redirection are found
when operating the tilted or yawed turbines at higher axial induction.

70 The formulation of the problem at hand is introduced in §2. Results are reported in §3 and further discussed in §4. Additional
details on used methods are provided in the appendix.

2 Problem formulation

We address the case of two spanwise-periodic rows of wind turbines immersed in a neutral atmospheric boundary layer (ABL)
at latitude 41°N . The flow is simulated by means of large-eddy simulations (LES) with SOWFA (see Appendix A and Church-
75 field et al., 2012, for additional details).

NREL 5-MW turbines (Jonkman et al., 2009) are considered, which are modeled with SOWFA's native actuator disk method
where wake rotation, the radial distribution of aerodynamic forces and the thrust coefficient are all computed from blade proper-
ties providing a reliable descriptions of the wake structure except in the near-wake region. We also make use of SOWFA's native
implementation of NREL 5-MW's realistic five-region turbine controller based on generator-torque control in the Region-II
80 regime corresponding to the mean wind speeds considered in the following; in this regime we modify axial induction by chang-
ing the rotor-collective blade pitch angle β . Higher axial inductions are obtained by enforcing negative values of β , resulting in
higher local thrust coefficients $C'_T = 2T/(\pi\rho u_n^2 A)$, where T is the thrust magnitude and u_n is the disk-averaged wind velocity
component normal to the disk of area $A = \pi D^2/4$.

The incoming flow, generated by means of a precursor simulation in a $3\text{km} \times 3\text{km}$ domain in the absence of turbines,
85 has a 100m-thick capping-inversion layer centered at $H=750\text{m}$ separating the neutral boundary layer with constant poten-
tial temperature ($\theta=300\text{K}$) from the geostrophic region above where the vertical potential temperature gradient is positive
($d\theta/dz)_G = 0.03\text{K}/\text{m}$). In the capping-inversion layer this gradient is $(d\theta/dz)_{CI} = 0.03\text{K}/\text{m}$. In the precursor simulation,
the ABL is driven by a pressure gradient adjusted to maintain an horizontally-averaged mean of 8m/s from the west at $z=100\text{m}$
(a few meters above hub height $z_h=89\text{m}$). In the region spanned by the turbines ($z < 152\text{m}$) the streamwise mean velocity is
90 well approximated by the logarithmic law and the vertical wind veer is less than 4° (see Cossu, 2020b, where the same ABL
has been already considered).

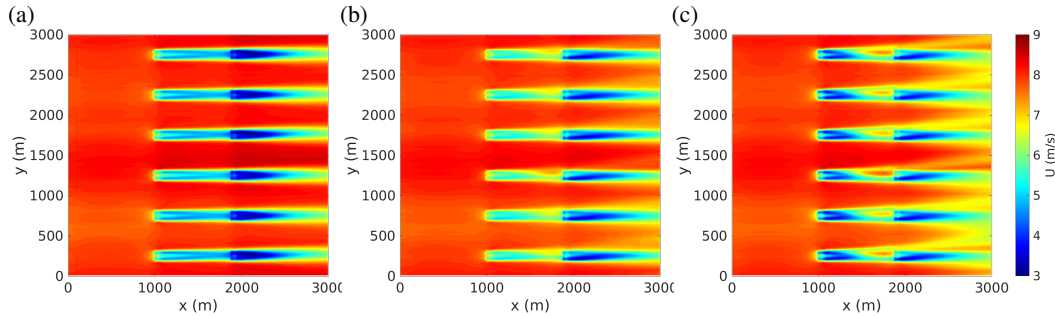


Figure 1. Tilt control: Mean (temporally averaged) streamwise velocity field in the horizontal plane at hub height obtained (a) in the baseline case where all turbines are operated in default mode, (b) with upwind turbines tilted by $\varphi = 30^\circ$ and operated at the default rotor-collective blade pitch angle $\beta = 0^\circ$ and (c) with upwind turbines tilted by $\varphi = 30^\circ$ and operated at higher induction ($\beta = -5^\circ$). The mean wind is from the west (from the left, parallel to the x axis).

Simulations in the presence of wind turbines are repeated in the same 3km x 3km domain starting from the solution of the precursor simulation at $t_0=20000$ s, corresponding to a well developed ABL, up to $t_1=30000$ s. Statistics are computed starting from $t=24000$ s, when turbine wakes are fully developed. The pressure gradient issued from the precursor simulation is enforced during the simulation with turbines and the (previously stored) ABL solution at $x=0$ (west boundary) is used as inflow boundary condition.

In each (spanwise-periodic) row, turbines are spaced by $4D$ in the spanwise direction (where $D=126$ m is the rotor diameter) and the two rows, are spaced by $7D$ in the streamwise direction with corresponding turbines of each row aligned with respect to the mean-wind direction (see Fig. 1). Downwind-row turbines are always operated in default mode with the rotor axis at zero yaw angle $\gamma = 0^\circ$ (aligned with the mean wind), tilt angle $\varphi = -5^\circ$ (to prevent rotor-tower hits) and rotor-collective blade pitch angle $\beta = 0^\circ$. In the baseline (reference) case upwind-row turbines are also operated in default mode. The baseline case is then compared to a set of controlled cases where all the turbines of the upwind row are operated at the same non-zero tilt or yaw angle and, possibly, non-zero pitch angle.

3 Results

3.1 Effect of overinduction on tilt control

In the baseline case (all turbines operated with $\gamma = 0^\circ$, $\varphi = -5^\circ$, $\beta = 0^\circ$), the usual situation is found where the turbines of the downwind row see a strongly reduced mean wind (see Fig. 1a) therefore producing only $\approx 30\%$ of the total power, i.e. $\approx 40\%$ of the produced by the upwind row of turbines (see Fig. 2b). In the following, power gains will be computed with respect to the mean power P_{Ref} produced in this baseline case.

We then consider the case where upwind-row turbines are tilted by $\varphi = 30^\circ$, an angle in the range where best power gains have been found in previous studies (Fleming et al., 2014, 2015; Cossu, 2020a, b), while keeping their rotor-collective blade

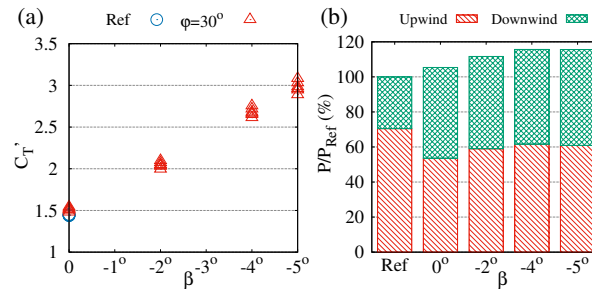


Figure 2. Effect of enforcing negative rotor-collective blade pitch angles β on upwind-row turbines tilted by $\varphi = 30^\circ$. Panel (a): (temporally-averaged) local thrust coefficient C_T' of the individual turbines of the upwind row. Panel (b) wind power extracted by the upwind (hatched red) and downwind (cross-hatched green) rows of turbines normalized by the total power P_{Ref} produced in the baseline case (Ref).

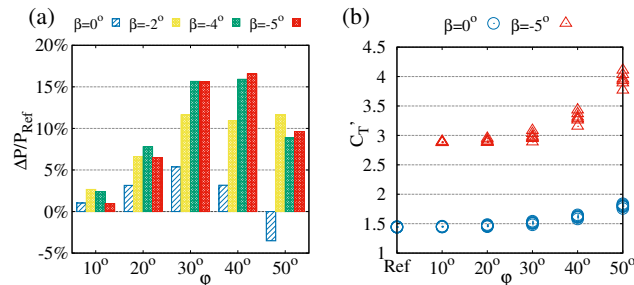


Figure 3. Effect of the tilt angle φ on: (a) the total power gain $(P - P_{Ref})/P_{Ref}$ for selected values of β ; (b) the local thrust coefficients C_T' of upwind-row turbines when they are operated with $\beta = 0^\circ$ (default axial induction) or with $\beta = -5^\circ$ (strongly overinductive regime).

pitch angle at the default value $\beta = 0^\circ$. In this case, the wakes of the upwind turbines are pushed down by the tilt-induced downwash increasing the mean wind available to downwind turbines (see Fig. 1b). The tilt-induced decrease of power produced by upwind-row turbines is compensated by the increase of the power produced by downwind-row turbines resulting in an $\approx 5\%$ global power gain for $\varphi = 30^\circ$ tilt angles (see Fig. 2b).

In a further step, the rotor-collective blade pitch angle of the tilted upwind-row turbines is changed. Enforcing increasingly negative values of β (i.e. increasing the mean angle of attack of all rotor blades) results in increased thrust coefficients (increased axial induction) which, starting from $C_T' = 1.5$ in the baseline case ($\beta = 0^\circ$), attain $C_T' = 3$ for $\beta = -5^\circ$ in turbines tilted by $\varphi = 30^\circ$ (see Fig. 2a). The effect of the increased thrust is twofold: it reinforces the downwash, further increasing the available wind and extracted power in downwind turbines despite the higher wake deficit of upwind turbines (compare Fig. 1c to Fig. 1b) but it also (more slightly) increases the power produced by tilted turbines (Fig. 2b). The combination of these two effects results in highly enhanced (almost tripled) power gains.

Finally, a full set of φ - β combinations is considered. From Fig. 3a it can be seen that tilt-induced power gains are highly enhanced (more than doubled) even with the moderate rotor-collective blade pitch angle $\beta = -2^\circ$ and that optimal β values do depend on φ ($\beta = -2^\circ$ is the best for $\varphi = 10^\circ$, $\beta = -4^\circ$ is the best one for $\varphi = 20^\circ$, while $\beta = -5^\circ$ appears well adapted for $\varphi \gtrsim 30^\circ$). Maximum power gains are reached for $\varphi \approx 40^\circ$, a value larger than the optimal $\varphi \approx 30^\circ$ found when $\beta = 0^\circ$.

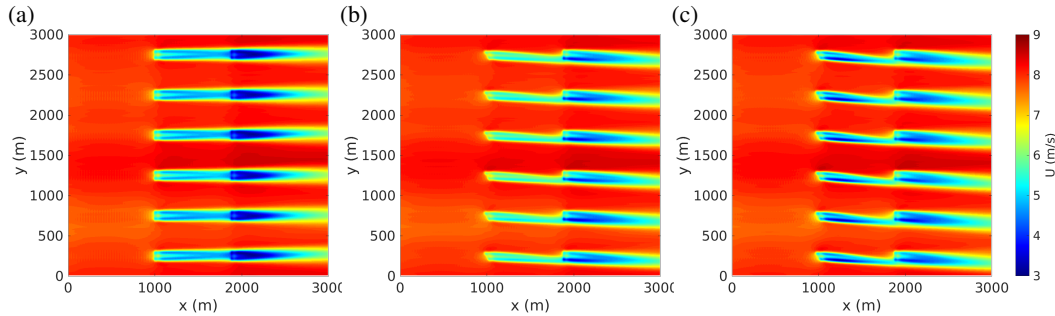


Figure 4. Yaw control: Mean streamwise velocity field in the horizontal plane at hub height obtained (a) in the baseline case where all turbines are operated in default mode ($\gamma = 0^\circ$, $\beta = 0^\circ$ same as Fig. 1a, reproduced here to ease the comparison), (b) in the case with upwind turbines yawed by $\gamma = 30^\circ$ and operated at the default $\beta = 0^\circ$ and (c) with upwind turbines yawed by $\gamma = 30^\circ$ and operated at higher induction ($\beta = -5^\circ$).

This is probably related to the fact that for a selected fixed value of β , the local thrust coefficient C'_T remains almost constant with the tilt angle up to $\varphi \approx 30^\circ$ but increases for higher values of φ (see Fig. 3b) leading to a stronger downwash which more efficiently exploits the vertical velocity gradient. Smaller values of the optimal tilt angle φ would probably be found if C'_T was held constant instead of β (as in Cossu, 2020b).

Contrary to a first intuition, increasing the local thrust coefficient C'_T is not an issue for mean turbine loads because turbines are tilted. Indeed, when turbines are tilted at the default $\beta = 0^\circ$, their mean load (essentially the thrust force) decreases because of the reduced incoming mean wind u_n normal to the rotor. For the considered cases, the increase of C'_T obtained with negative values of β counteracts this thrust decrease but the thrust magnitude remains almost unchanged (within 5%) with respect to the baseline case for $\varphi \lesssim 30^\circ$ when optimal β values are used for each φ and is reduced for larger φ values (not shown). Thrust magnitudes exceed that of the baseline case by more than 5% only when a (suboptimal) excessive induction is enforced for $\varphi \lesssim 20^\circ$. Note also, that in tilted turbines an important part of the thrust force is directed along the (positive) vertical direction compensating the gravity force; the remaining horizontal part of the thrust force is therefore always reduced in turbines operated at the optimal β .

140 3.2 Effect of overinduction on yaw control

To evaluate the effect of overinductive operation on yaw control we proceed similarly to the tilt-control case by using the same precursor simulation and the same baseline case where all turbines operate at default values $\gamma = 0^\circ$, $\varphi = -5^\circ$, $\beta = 0^\circ$. We first simulate the standard yaw control where the yaw angle γ of upwind-row turbines is changed (while keeping unchanged the other parameters $\varphi = -5^\circ$, $\beta = 0^\circ$) resulting in the well known horizontal deviation of upwind-row turbine wakes and the increase of the mean wind speed seen by downwind rotors (see Fig. 4b). From Fig. 5b it is seen that, in this case, the increase of the power produced by downwind-row turbines compensates the reduction of the power produced by the yawed (upwind-row) resulting in maximum power gains of $\approx 5\%$ obtained for $\gamma = 20^\circ - 30^\circ$ (see Fig. 6a), similarly to the values found by Fleming et al. (2015) for the two-turbines case.

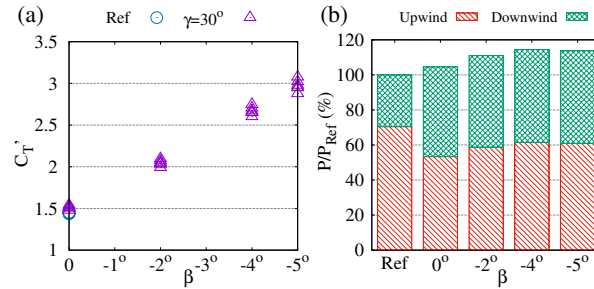


Figure 5. Effect of changing the rotor-collective blade pitch angle β of turbines yawed by $\gamma = 30^\circ$. Panel (a): local thrust coefficient C_T' of the turbines of the upwind row. Panel (b): wind power extracted by the upwind (hatched red) and downwind (cross-hatched green) rows of turbines normalized by the total power P_{Ref} extracted in the baseline case.

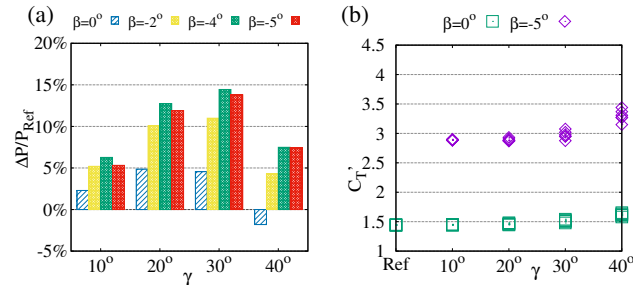


Figure 6. Effect of the yaw angle γ on (a) power gains for selected values of rotor-collective blade pitch angle β and (b) on the local thrust coefficients C_T' of upwind-row turbines when they are operated at $\beta = 0^\circ$ or at $\beta = -5^\circ$.

Increasing the local thrust coefficient C_T' by means of increasingly negative blade-pitch angles in yawed turbines (see Fig. 5a) has effects similar to those observed for the tilt-control case: an increase of wake deficits in upwind-row turbine wakes but also their higher deviation away from downwind turbines (see Fig. 4c) resulting in an increase of the mean power produced by all turbines (Fig. 5b) with respect to the standard yaw-control case with $\beta = 0^\circ$.

The analysis of power gains obtained with different γ - β combinations, reported in Fig. 6a, reveals that global power gains obtained by yaw control are highly enhanced when yawed turbines are operated at higher induction. Power gains are indeed more than doubled already for $\beta = -2^\circ$ and are almost tripled for the optimal yaw-pitch combination $\gamma = 30^\circ$, $\beta = -4^\circ$.

Similarly to the tilt-control case, at higher induction the optimal yaw angles are higher ($\gamma \approx 30^\circ$) than in the standard yaw-control case ($\gamma \approx 20^\circ$ for $\beta = 0^\circ$). However, differently from the tilt control case, the optimal pitch angle is not very sensitive to the yaw angle, $\beta = -4^\circ$ being the optimal value for all considered tilt angles and the increase of C_T' observed for $\gamma \gtrsim 30^\circ$ (see Fig. 6b) does not result in a shift of optimal yaw angles to values larger than 30° even for the highest considered $\beta = -5^\circ$. This can be probably explained by observing that the vertical wind shear is not exploited by yaw control and thus, in the yaw-control case very large wake deviations are less beneficial than in the tilt-control case.



4 Conclusions

The main goal of this study was to assess the magnitude of global power gains that can be obtained in wind turbine arrays by combining static wake redirection control and static axial induction control operating tilted or yawed turbines at higher axial induction (overinduction). Results have been obtained by means of large-eddy simulations of a two-rows array of NREL 5MW turbines in a neutral atmospheric boundary layer.

In a first part of the study we have considered the effect of higher induction on tilt-control by using an actuator disk model less idealized than the one used in our previous studies of this approach. The results confirm that, also with this more realistic turbine model, power gains can be highly increased by operating tilted turbines at higher induction (power gains above 15% are found, to be compared to $\approx 5\%$ obtained with default induction, for the considered set of parameters). This substantial enhancement of power gains is consistent with those found in our previous studies (the absolute level of power gains was, however, larger in Cossu (2020a, b) where three rows of turbines were considered instead of the two rows considered here). It is also found that rotor-collective blade pitch angles β (and therefore local thrust coefficients C'_T) maximizing global power gains do increase with the rotor tilt angle φ suggesting that an optimized law $\beta(\varphi)$ depending on the specific turbine design should be used in tilt-control operation. Our result also indicate that the use of such an optimized law would also guarantee that the thrust magnitude in overinductive tilt-control does not exceed the one of the baseline case by more than 5%.

In the second part of the study we have ascertained if the overinductive wake redirection approach results in power gain enhancement also in the case of yaw control. To this end, we have first considered the standard case where yaw turbines are operated at the standard $\beta = 0$ finding power gains of the order of 5%, similar to those found in numerous previous studies (e.g. Fleming et al., 2015, for the two-turbines case). We then show that a very significant increase of power gains (almost threefold, up to $\approx 15\%$ for the cases considered) is obtained by operating yawed turbines at higher induction.

The findings concerning overinductive yaw control are probably the most relevant of this study. They could, indeed, provide an explanation for the high power gains found by Park and Law (2015) and Munters and Meyers (2018) (by means advanced optimization techniques where both yaw angles and axial inductions were used as control variables) showing that similar power gains can be realized with simple static open-loop overinductive yaw control in a realistic model (the atmospheric boundary layer with NREL 5-MW turbines simulated with SOWFA). Furthermore, yaw control can be tested and applied in most of currently installed wind farms, unlike tilt control which is promising for specifically designed future generation downwind-oriented and/or floating turbines (Bay et al., 2019; Nanos et al., 2020).

Additional investigations are, however, necessary to further refine, in many directions, the conclusions of the present study. Quantitative refinements based on higher-fidelity simulations making use of the actuator line method, and necessarily more refined grids, would be welcome, especially for the largest considered values of the yaw, tilt and pitch angles where the near- and middle-wake structure is probably more sensitive to details of the turbine model.

Another issue is the wind direction. The present study is limited to the wind-aligned case, but it is, of course, important to evaluate power gains also in non-aligned configurations. In this context, an improvement of existing simplified wake models



195 in high-tilt/yaw and pitch angles regime would make possible a more precise prediction of annual energy production gains obtained with overinductive yaw or tilt control for realistic wind roses and wind farm configurations.

Finally, it would be very interesting to ascertain if additional power gain enhancements could come from the simultaneous activation of tilt, yaw and axial induction control. It might indeed be possible that, as a consequence of the symmetry breaking associated to wake rotation effects and Coriolis acceleration, optimal power gains are obtained with “hybrid” yaw-tilt rotor-axis
200 rotations even in wind-aligned configurations. This is the subject of current intense research effort.

Appendix A: Methods

Large-eddy simulations are performed with SOWFA (the Simulator for On/Offshore Wind Farm Applications developed at NREL, see Churchfield et al., 2012). SOWFA is based on OpenFOAM, which solves partial differential equations based on a finite-volume framework (Jasak, 2009; OpenCFD, 2011). The filtered Navier-Stokes equations are solved using Smagorinsky
205 (1963) model to approximate subgrid-scale stresses. Compressibility effects are included with the Boussinesq approximation and the horizontal component of Coriolis acceleration is included in the equations. Schumann (1975) stress boundary conditions, modeling the effect of ground roughness, are applied near the ground and slip boundary conditions are enforced at the top of the solution domain. The solutions are advanced in time using the PIMPLE scheme.

Periodic boundary conditions are applied in the x (west-east) direction for the preliminary ‘precursor’ simulations where
210 the atmospheric boundary layer flow is computed in the absence of wind turbines in order to generate realistic inflow wind conditions (Keating et al., 2004; Tabor and Baba-Ahmadi, 2010; Churchfield et al., 2012). The mean pressure gradient is adapted in order to maintain a (horizontally-averaged) mean westerly 8m/s wind at $z = 100m$. The time-history of the mean pressure gradient and of the solution at $x = 0$ are stored and then used in the simulations with wind turbines which are run in the same domain with the same grid but removing the periodicity constraint in the streamwise direction and replacing it with
215 an inflow condition enforcing the solution found $x = 0$ in the precursor simulation. Periodic boundary conditions are applied in the y (south-north) direction for both precursor simulations and simulations with turbines.

The solution domain extends 1km in the vertical direction and 3km x 3km along the x and y axes and is discretized with cells extending 15m x 15m in the x and y directions and 7m (near the ground) to 21m (near the top boundary) in the vertical direction. $\Delta t = 0.8s$ time steps are used to advance the solution. These parameters keep manageable the amount of data stored
220 in the precursor simulation.

The aerodynamics forces on NREL 5-MW turbines, having a $D=126m$ rotor diameter and $z_h=89m$ hub height (Jonkman et al., 2009), are modeled with SOWFA’s native actuator disk method where aerodynamic forces are computed from the characteristics of NREL 5-MW blade profiles, rotational speed and the resolved wind velocity. A Gaussian projection of the discretized body forces with a smoothing parameter $\varepsilon = 20m$ is also used to avoid numerical instabilities (Martínez-Tossas and
225 Leonardi, 2013). The NREL 5-MW five-region controller implemented in SOWFA is used to control the turbines rotational speed and axial induction. In the Region II regime, the one accessed in the presented simulation, the turbine is driven to the design point (tip-speed ratio and thrust coefficient corresponding to the maximum power coefficient for an isolated turbine)



by means of generator-torque control at the default rotor-collective blade pitch angle $\beta = 0^\circ$. In this regime, the static axial induction control is applied by changing the rotor-collective blade pitch angle β while leaving unchanged the other parameters of the generator torque controller.

The local thrust coefficient is retrieved from the computed turbine thrust magnitude and rotor-averaged normal mean wind speed u_n by making use of its definition $C'_T = 8T / \pi \rho u_n^2 D^2$.

Competing interests. The author declares no conflict of interest.

Acknowledgements. I gratefully acknowledge the use of the Simulator for On/Offshore Wind Farm Applications (SOWFA) developed at NREL (Churchfield et al., 2012) based on the OpenFOAM finite volume framework (Jasak, 2009; OpenCFD, 2011).



References

- Annoni, J., Gebraad, P. M. O., Scholbrock, A. K., Fleming, P. A., and van Wingerden, J.-W.: Analysis of Axial-Induction-Based Wind Plant Control Using an Engineering and a High-Order Wind Plant Model, *Wind Energy*, 19, 1135–1150, <https://doi.org/10.1002/we.1891>, <http://doi.wiley.com/10.1002/we.1891>, 2016.
- 240 Bastankhah, M. and Porté-Agel, F.: Experimental and Theoretical Study of Wind Turbine Wakes in Yawed Conditions, *J. Fluid Mech.*, 806, 506–541, <https://doi.org/10.1017/jfm.2016.595>, https://www.cambridge.org/core/product/identifier/S0022112016005954/type/journal_article, 2016.
- Bay, C. J., Annoni, J., Martínez-Tossas, L. A., Pao, L. Y., and Johnson, K. E.: Flow Control Leveraging Downwind Rotors for Improved Wind Power Plant Operation, in: 2019 American Control Conference (ACC), pp. 2843–2848, IEEE, 2019.
- 245 Boersma, S., Doekemeijer, B., Gebraad, P., Fleming, P., Annoni, J., Scholbrock, A., Frederik, J., and van Wingerden, J.-W.: A tutorial on control-oriented modeling and control of wind farms, in: 2017 American Control Conference (ACC), pp. 1–18, IEEE, <https://doi.org/10.23919/ACC.2017.7962923>, <http://ieeexplore.ieee.org/document/7962923/>, 2017.
- Calaf, M., Meneveau, C., and Meyers, J.: Large Eddy Simulation Study of Fully Developed Wind-Turbine Array Boundary Layers, *Phys. Fluids*, 22, 015 110, <https://doi.org/10.1063/1.3291077>, <http://aip.scitation.org/doi/10.1063/1.3291077>, 2010.
- 250 Campagnolo, F., Petrović, V., Schreiber, J., Nanos, E. M., Croce, A., and Bottasso, C. L.: Wind Tunnel Testing of a Closed-Loop Wake Deflection Controller for Wind Farm Power Maximization, *J. Phys. Conf. Ser.*, 753, 032 006, <https://doi.org/10.1088/1742-6596/753/3/032006>, <https://iopscience.iop.org/article/10.1088/1742-6596/753/3/032006>, 2016.
- Churchfield, M. J., Lee, S., Michalakes, J., and Moriarty, P. J.: A Numerical Study of the Effects of Atmospheric and Wake Turbulence on Wind Turbine Dynamics, *J. Turbul.*, 13, N14, <https://doi.org/10.1080/14685248.2012.668191>, <http://www.tandfonline.com/doi/abs/10.1080/14685248.2012.668191>, 2012.
- 255 Cossu, C.: Replacing wakes with streaks in wind turbine arrays, *Wind Energy* (to appear), <https://arxiv.org/pdf/2007.01617>, 2020a.
- Cossu, C.: Evaluation of tilt control for wind-turbine arrays in the atmospheric boundary layer, *Wind Energy Sci.* (sub judice), <https://doi.org/10.5194/wes-2020-106>, 2020b.
- Dahlberg, J. Å. and Medici, D.: Potential improvement of wind turbine array efficiency by active wake control (AWC), in: Proc. European Wind Energy Conference, European Wind Energy Association, Madrid, Spain, 2003.
- 260 Fleming, P., Gebraad, P. M., Lee, S., van Wingerden, J.-W., Johnson, K., Churchfield, M., Michalakes, J., Spalart, P., and Moriarty, P.: Simulation Comparison of Wake Mitigation Control Strategies for a Two-Turbine Case, *Wind Energy*, 18, 2135–2143, <https://doi.org/10.1002/we.1810>, 2015.
- Fleming, P. A., Gebraad, P. M., Lee, S., van Wingerden, J.-W., Johnson, K., Churchfield, M., Michalakes, J., Spalart, P., and Moriarty, P.: Evaluating Techniques for Redirecting Turbine Wakes Using SOWFA, *Renew. Energy*, 70, 211–218, <https://doi.org/10.1016/j.renene.2014.02.015>, <https://linkinghub.elsevier.com/retrieve/pii/S0960148114000950>, 2014.
- 265 Goit, J. P. and Meyers, J.: Optimal Control of Energy Extraction in Wind-Farm Boundary Layers, *J. Fluid Mech.*, 768, 5–50, <https://doi.org/10.1017/jfm.2015.70>, http://www.journals.cambridge.org/abstract_S0022112015000701, 2015.
- Howland, M. F., Bossuyt, J., Martínez-Tossas, L. A., Meyers, J., and Meneveau, C.: Wake Structure in Actuator Disk Models of Wind Turbines in Yaw under Uniform Inflow Conditions, *J. Renew. Sustain. Energy*, 8, 043 301, <https://doi.org/10.1063/1.4955091>, 2016.
- 270 Jasak, H.: OpenFOAM: open source CFD in research and industry, *Int. J. Naval Arch. Oc. Eng.*, 1, 89–94, 2009.



- Jiménez, A., Crespo, A., and Migoya, E.: Application of a LES Technique to Characterize the Wake Deflection of a Wind Turbine in Yaw, *Wind Energy*, 13, 559–572, <https://doi.org/10.1002/we.380>, <http://doi.wiley.com/10.1002/we.380>, 2010.
- Jonkman, J., Butterfield, S., Musial, W., and Scott, G.: Definition of a 5-MW reference wind turbine for offshore system development, Technical Paper NREL/TP-500-38060, National Renewable Energy Lab.(NREL), Golden, CO (United States), 2009.
- 275 Keating, A., Piomelli, U., Balaras, E., and Kaltenbach, H.-J.: A priori and a posteriori tests of inflow conditions for large-eddy simulation, *Phys. fluids*, 16, 4696–4712, <https://doi.org/10.1063/1.1811672>, 2004.
- Knudsen, T., Bak, T., and Svenstrup, M.: Survey of wind farm control-power and fatigue optimization: Survey of wind farm control, *Wind Energy*, 18, 1333–1351, <https://doi.org/10.1002/we.1760>, <http://doi.wiley.com/10.1002/we.1760>, 2015.
- 280 Martínez-Tossas, L. and Leonardi, S.: Wind Turbine Modeling for Computational Fluid Dynamics, Subcontract Report NREL/SR-5000-55054, US National Renewable Energy Laboratory, Golden, CO (USA), 2013.
- Medici, D. and Alfredsson, P. H.: Measurements on a Wind Turbine Wake: 3D Effects and Bluff Body Vortex Shedding, *Wind Energy*, 9, 219–236, <https://doi.org/10.1002/we.156>, <http://doi.wiley.com/10.1002/we.156>, 2006.
- Munters, W. and Meyers, J.: An Optimal Control Framework for Dynamic Induction Control of Wind Farms and Their Interaction with the Atmospheric Boundary Layer, *Philos. Trans. R. Soc. Math. Phys. Eng. Sci.*, 375, 20160100, <https://doi.org/10.1098/rsta.2016.0100>, <http://rsta.royalsocietypublishing.org/lookup/doi/10.1098/rsta.2016.0100>, 2017.
- 285 Munters, W. and Meyers, J.: Dynamic Strategies for Yaw and Induction Control of Wind Farms Based on Large-Eddy Simulation and Optimization, *Energies*, 11, 177, <https://doi.org/10.3390/en11010177>, <http://www.mdpi.com/1996-1073/11/1/177>, 2018.
- Nanos, E. M., Letizia, S., Barreiro Clemente, D. J., Wang, Cand Rotea, M., Iungo, V. I., and Bottasso, C. L.: Vertical wake deflection for offshore floating wind turbines by differential ballast control, in: *J. Phys: Conf. Series*, vol. 1618, p. 022047, IOP Publishing, <https://doi.org/10.1088/1742-6596/1618/2/022047>, 2020.
- OpenCFD: OpenFOAM - The Open Source CFD Toolbox – User’s Guide, OpenCFD Ltd., UK, 2.4 edn., <http://www.openfoam.org>, 2011.
- Park, J. and Law, K. H.: Cooperative Wind Turbine Control for Maximizing Wind Farm Power Using Sequential Convex Programming, *Energy Convers. Manag.*, 101, 295–316, <https://doi.org/10.1016/j.enconman.2015.05.031>, <https://linkinghub.elsevier.com/retrieve/pii/S0196890415004781>, 2015.
- 295 Porté-Agel, F., Bastankhah, M., and Shamsoddin, S.: Wind-Turbine and Wind-Farm Flows: A Review, *Bound.-Layer Meteorol.*, <https://doi.org/10.1007/s10546-019-00473-0>, <http://link.springer.com/10.1007/s10546-019-00473-0>, 2019.
- Schumann, U.: Subgrid scale model for finite difference simulations of turbulent flows in plane channels and annuli, *J. Comp. Phys.*, 18, 376–404, [https://doi.org/10.1016/0021-9991\(75\)90093-5](https://doi.org/10.1016/0021-9991(75)90093-5), 1975.
- 300 Shapiro, C. R., Gayme, D. F., and Meneveau, C.: Modelling Yawed Wind Turbine Wakes: A Lifting Line Approach, *J. Fluid Mech.*, 841, <https://doi.org/10.1017/jfm.2018.75>, https://www.cambridge.org/core/product/identifier/S0022112018000757/type/journal_article, 2018.
- Smagorinsky, J.: General circulation experiments with the primitive equations: I. The basic experiment, *Mon. Weather Rev.*, 91, 99–164, [https://doi.org/10.1175/1520-0493\(1963\)091<0099:GCEWTP>2.3.CO;2](https://doi.org/10.1175/1520-0493(1963)091<0099:GCEWTP>2.3.CO;2), 1963.
- Steinbuch, M., De Boer, W., Bosgra, O., Peeters, S., and Ploeg, J.: Optimal control of wind power plants, *J. Wind Eng. Ind. Aerodyn.*, 27, 237–246, 1988.
- 305 Stevens, R. J. and Meneveau, C.: Flow Structure and Turbulence in Wind Farms, *Annu. Rev. Fluid Mech.*, 49, 311–339, <https://doi.org/10.1146/annurev-fluid-010816-060206>, <http://www.annualreviews.org/doi/10.1146/annurev-fluid-010816-060206>, 2017.
- Tabor, G. R. and Baba-Ahmadi, M. H.: Inlet conditions for large eddy simulation: A review, *Computers & Fluids*, 39, 553–567, <https://doi.org/10.1016/j.compfluid.2009.10.007>, 2010.